Investigating the phytoplankton diversity in the Great Calcite Belt: perspective from modelling and satellite retrievals

Svetlana N. Losa[1]*, Julia Oelker*[2]*, Mariana A. Soppa*[1]*, Stephanie Dutkiewicz*[3]*, Martin Losch*[1]*,*
Tilman Dinter[1]*, Andreas Richter*[2]*, Vladimir V. Rozanov*[2]*, John P. Burrows*[2]*, Astrid Bracher*[1,2]

[1]*Alfred Wegener Institute Helmholtz Centre for Polar and Marine Research, Bremerhaven, Germany*
[2] *Institute of Environmental Physics (IUP), University of Bremen, Bremen, Germany*
[3]*Massachusetts Institute of Technology, Cambridge, Massachusetts, USA*

Abstract

This study highlights benefits and challenges of applying coupled physical/biogeochemical modeling and the synergistic use of different satellite retrieval algorithms for investigating the phytoplankton diversity in the Great Calcite Belt. This area is of great interest for understanding biogeochemical cycling and ecosystem functioning under present climate changes observed in the Southern Ocean. Our coupled model simulations of the phenology of various Phytoplankton Functional Types (PFTs) are based on a version of the Darwin biogeochemical model (Dutkiewicz et al., 2015) coupled to the MITgcm circulation model (MITgcm Group, 2012), in which both - the physical and biogeochemical modules - are adapted for the Southern Ocean. As satellite-based PFT information, we consider products of the PhytoDOAS (Bracher et al. 2009, Sadeghi et al. 2012) using SCIAMACHY, OMI, GOME-2 hyper-spectral optical satellite measurements. We also address aspects of combining this information synergistically (SynSenPFT, Losa et al. 2017) with the phytoplankton composition retrieved with OC-PFT (Hirata et al. 2011, Soppa et. al. 2014, 2016) based on multi-spectral optical satellite data (OC-CCI) and obtained by numerical modelling to allow for long time-series on the Southern Ocean phytoplankton diversity. To evaluate the satellite retrievals and model simulations we use *in situ* PFTs obtained a diagnostic pigment analysis (Soppa et al., 2017) as well as by scanning electron microscopy (Smith et al., 2017).

1 Method

1.1 Remote sensing

1.1.1 Hyper-spectral-based retrievals

Chlorophyll *"a"* concentration (Chla) of important phytoplankton groups in the Southern Ocean (including biomineralizing phytoplankton types observed in the Great Calcite Belt) are derived using differential optical absorption spectroscopy (PhytoDOAS, Bracher et al. 2009, Sadeghi et al. 2012, Bracher et al. 2017: doi.org/10.1594/PANGAEA.870486) on hyperspectral satellite data. One of the sources of hyperspectral information is the Scanning Imaging Absorption Spectrometer for Atmospheric Chartography (SCIAMACHY) available till 2012. These observations were complemented by adapting PhytoDOAS to the current satellite hyperspectral measurements from the Ozone Monitoring Instrument (OMI) and Global Ozone Monitoring Experiment – 2 (GOME-2, operationally providing data from 2007 on until present and in the future). OMI can also bridge the gap until 2018 when its successor the TROPOspheric Monitoring Instrument (TROPOMI) has been launched on Sentinel-5. Combining the PFT products from different hyper-spectral sensors provides better spatial sampling of the Southern Ocean (the Great Calcite Belt, in particular) and enables the extension of observed time period (2002 until present).

1.1.2 Synergistic combination of hyper- and multispectral information

The hyperspectral satellite PFT retrievals were synergistically combined with information derived from multi-spectral measurements. In the study by Losa et al (2017) satellite retrievals of chlorophyll “a” concentrations Chla for diatom, coccolithophores, cyanobacteria were derived based on a synergistic use (SynSenPFT, Losa et al., 2017) of multi-spectral-based (Soppa et al. 2014) and hyper-spectral-based (Bracher et al. 2009, Sadeghi et al. 2012) phytoplankton absorption information via optimal interpolation. In their study, the SynSenPFT diatom and coccolithophores Chla products were obtained with the PhytoDOAS method given SCIAMACHY hyperspectral measurements (Bracher et al. 2017) and OC-PFT abundance-based approach (Hirata et. al. 2011, Soppa et al. 2014) applied to multi-spectral OC-CCI total Chla retrievals. As proposed in the study by Losa et al. (2017), the SynSenPFT can be extended by including hyperspectral observation from various sensors as well as by assimilating information from numerical modelling.

1.2 Numerical Modeling

1.2.1 Biogeochemistry

Among 42 biogeochemical compartments describing ocean biogeochemical cycling of phosphorus (P), nitrogen (N), carbon (C), oxygen(O), silicon (Si) and iron (Fe) (see Figure 1), the version of the Darwin model used in our study simulates 6 various phytoplankton functional types. In the original version of the model, they are analogues of diatoms, other micro-phytoplankton, prochlorophytes, other pico-phytoplankton, nitrogen fixing PFTs (incl. *Trichodesmium*) and coccolithophores. To adapt the Darwin model for plausible simulations of the Southern Ocean biogeochemistry and phytoplankton dynamics and diversity, the following steps were executed:

- assumed coccolithophores physiology were corrected to account for high affinity for nutrients, immune to photoinhibition (Tyrrell and Taylor, 1996) and ability to escape grazing control (Huskin et al. 2000, Nejstgaard et al. 1997);
- Southern Ocean diatom diversity was represented by two distinct size classes introduced for diatoms (as two different model variables): smaller and “slightly silicified and fast growing” at lower latitudes larger and “strongly silicified slowly growing cells” at high latitudes (Quéguiner 2013);
- several sensitivity experiments were performed to investigate the possibility to simulate realistically co-existence of coccolithophores and *Phaeocystis sp.(ant.).*

1.2.2 Physics

The biogeochemical model was coupled with the MITgcm circulation model (MITgcm Group, 2012) based on a cubed-sphere grid (Menemenlis et al. 2008) with mean horizontal spacing of ~18 km and 50 vertical levels with the resolution ranging from 10 m near the surface to ~450 m in the deep ocean (as in Taylor et al., 2013). In the sea-ice model no replacement pressure was used (Kimmritz et al. 2017). The model was forced by 3-hourly atmospheric conditions from the Japanese 55-year reanalysis (JRA55) over the time period of 1999 – 2010 following a spin up period 1992 – 1998.

2 Results

2.1 Satellite retrievals

2.1.1 Comparison of hyper-spectral-based retrievals

Figure 2 shows spatial distribution of the PhytoDOAS coccolithophores fit factors retrieved from SCIAMACHY (upper panels), OMI (middle panels) and GOME-2 (bottom panels) for the Great Calcite Belt and averaged over the time period when the observations reported by Smith et al. (2017) were collected: 17 January – 17 February 2011 and 18 February – 20 March 2012. The SCIAMACHY-based spatial distribution agreed with those published by Smith et al. (2017) for coccolithophores. This distribution is also partly distinguishable in the GOME-2 retrievals (bottom panels), even though the initial spectral information is coming from larger ground pixels (80 x 40 km^2) then in case of SCIAMACHY (30 x 60 km^2). Evaluation of OMI-based fit factor (13 x 24 km^2) indicated difficulties in retrieving because of the sensor degradation beginning 2008. One can also note the offset in the fit factors derived from GOME-2 measurements when comparing with SCIAMACHY-based retrievals. Further corrections for instrumental effects on the fit results are necessary to finally merge these data sets. These involve also the hyperspectral data products of vibrational Raman scattering which are necessary inputs to account for the penetration depth to which the satellites captures information. This varies from sensor to sensor and depends mainly on its solar zenith angle. When both corrections are finalised, a merge product can be produced.

2.1.2 SynSenPFT for the Great Calcite Belt

There are benefits of merging or synergistic combination of information from different sensors, either hyperspectral or hyper- and multispectral. Figure 3 depicts the Great Calcite Belt Chla for diatoms and coccolithophores, obtained by combining synergistically the SCIAMACHY hyperspectral-based PhytoDOAS product and the multi-spectral-based OC-PFT. The SynSenPFT for the Great Calcite Belt agrees well with diatom and coccolithophores from *in situ* abundance data by Smith at al. (2017, Figures 2, 3). The aforementioned co-existence of coccolithophores and diatoms in the GCB is also supported by our model simulations (Part 2.2). A similar Kalman-filter-based approach (SynSenPFT) is proposed to be applied for merging OMI, SCIAMACHY and GOME-2. The SynSenPFT algorithm will, however, require calibrating and increasing the radius of data influence to account for the gaps in OMI information because of the strong sensor degradation in 2008.

2.2 Darwin-MITgcm model simulations

2.2.1 General evaluation for the Southern Ocean

A series of Darwin-MITgcm experiments (with different model configurations with respect to assumed PFTs and their physiological parameters) have been conducted for the global ocean and evaluated for the Southern Ocean over the period of 1999 – 2010. The best simulations, in terms of agreement with observed phytoplankton composition and dominance (Trimborn et al., 2015; PHYSAT, Alvain et al. 2008) and diatom phenology (Soppa et al. 2016), were performed with prescribing two size classes of diatoms (large and small, Quéguiner 2013, Tréguer et al. 2018). Figure 4 illustrates model phytoplankton dominance obtained for June - August 2003, December 2003 and January – February 2004. One can notice significant improvement in the model PFT dominance agreement with PHYSAT data product when comparing to those previously reported (Dutkiewicz et al., 2015). These results suggest that the too early (relative to observations) appearance of diatom blooms in the Southern Ocean simulated by most (global ocean) biogeochemical models (as well in the Darwin model set up published in the study by Dutkiewicz et al. 2015) could be explained by their misrepresentation of diatom size diversity.

Figure 5 depicts time series of model chlorophyll “a” concentration (Chla) for micro-, nano- and pico-phytoplankton averaged over three biogeochemical provinces (Longhurst, 1998) located in the Southern Ocean. Micro-phytoplankton is presented by large diatoms, nano-phytoplankton – by haptophytes (coccolithophores and *Phaeocystis*), picophytoplankton also includes small diatoms. The figure also depicts (“stars”) *in situ* data available for provinces and time period (1999 - 2010). When comparing the presented model Chla of different phytoplankton types averaged within the biogeochemical provinces with *in situ* observations it is worth keeping in mind possible mismatches due to temporal and spatial representation (representation error) and differences in phytoplankton grouping (Bracher et al. 2017).

2.2.2 The model coccolithophores vs. diatoms in the Great Calcite Belt

The aforementioned augmentation of the biogeochemical module by diversity in diatom size appeared to be a prerequisite for the plausible simulation of the diatoms and coccolithophores in the Great Calcite Belt. Figure 6 shows the Southern Ocean spatial distribution of Chla for diatoms and haptophytes in January 2004, which is in a qualitative agreement with the observations by Signorini et al. (2006), Balch et al. (2016) and Smith et al. (2017). The figure illustrates the co-existence of model simulated diatoms and haptophytes as it observed in the Great Calcite Belt. It is worth, however, emphasizing that model representation of co-existence/competition within the haptophytes group (coccolithophores *vs. Phaeocystis*) still remain a challenge: small changes in Darwin model physiological parameters lead to outcompeting either *Phaeocystis* or coccolithophores. To cope with this “stochasticity”, we also introduced two distinct life stages of *Phaeocystis ant.* (colonies and solitary cells), depending on iron availability (Bender et al. 2018, Popova et al. 2007). The model *Phaeocystis* colonies escape grazing, have lower mortality and higher sinking rate in comparison with solitary cells (Popova et al. 2007). These results, however, need further evaluation (not shown).

3 Summary and Outlook

The observed co-existence of two different phytoplankton groups coccolithophores and diatoms in the Great Calcite Belt (Balch et al., 2016, Smith et al., 2017) is clearly distinguishable by the PhytoDOAS and SynSenPFT satellite retrievals and clearly simulated by the Darwin-MITgcm model adjusted for the Southern Ocean. This gives an opportunity to obtain long time series data to analyse/investigate the phenomena, its physical and biogeochemical drivers**.** Despite the OMI sensor degradation and large ground pixel size of GOME-2, the information assimilated with SynSenPFT (Losa et al. 2017) would allow to bridge the current and future satellite missions.

The Southern Ocean adjustment of the Darwin-MITgcm required introducing the diatom (size) diversity and corrected coccolithophores physiology, which might support a biochemical/physiological hypothesis on the GCB phenomena. Model sensitivity experiments however showed that further model developments are required to plausibly simulate co-existence of coccolithophores and *Phaeocystis*, since the competition within the haptophytes group still remains a delicate issue. This might propose additionally augmenting the Darwin model to account for changes in assumed size/life stage of *Phaeocystis ant.* (Popova et al. 2007, Moisan&Mitchell 2018, Bender et al. 2018).

4 Acknowledgement

The study was supported by DFG-Priority Program 1158 "Antarctic Research" (via “PhySyn” project); DFG Transregional Collaborative Research Centre TR 172 and Helmholtz Climate Initiative REKLIM (Regional Climate Change), a joint research project of the Helmholtz Association of German Research Centres (HGF). The SynSenPFT estimates and model simulations were obtained with resources provided by the North-German Supercomputing Alliance (HLRN).

5 References

Alvain, S., C. Moulin, Y. Dandonneau, and H. Loisel (2008), Seasonal distribution and succession of dominant phytoplankton groups in the global ocean: A satellite view, Global Biogeochem. Cycles, 22, GB3001, doi:10.1029/2007GB003154.

Bender, S. J., Moran, D. M., McIlvin, M. R., Zheng, H., McCrow, J. P., Badger, J., DiTullio, G. R., Allen, A. E., and Saito, M. A. (2018): Colony formation in *Phaeocystis antarctica*: connecting molecular mechanisms with iron biogeochemistry, Biogeosciences, 15, 4923-4942, https://doi.org/10.5194/bg-15-4923-2018.

Bracher, A., Bouman, H., Bricaud, A., Brewin, R. J. W., Brotas, V., Ciotti, A. M., Clementson, L., Devred, E., Di Cicco, A., Dutkiewicz, S., Hardman-Mountford, N. J., Hickman, A., Hieronymi, M., Hirata, T., Losa, S. N., Mouw, C. B., Organelli, E., Raitsos, D. E., Uitz, J., Vogt, M. and Wolanin, A. (2017): Obtaining Phytoplankton Diversity from Ocean Color: A Scientific Roadmap for Future Development., Frontiers in Marine Science, 4 (55). doi: 10.3389/fmars.2017.0005.

Bracher, A, Dinter, T., Wolanin, A., Rozanov, V. V., Losa, S., Soppa, M. A. (2017): Global monthly mean chlorophyll "a" surface concentrations from August 2002 to April 2012 for diatoms, coccolithophores and cyanobacteria from PhytoDOAS algorithm version 3.3 applied to SCIAMACHY data, https://doi.org/10.1594/PANGAEA.870486.

Bracher A., Vountas M., Dinter T., Burrows J.P., Röttgers R., Peeken I. (2009) Quantitative observation of cyanobacteria and diatoms from space using PhytoDOAS on SCIAMACHY data. Biogeosciences 6: 751–764.

Deppeler S. L. and Davidson A. T. (2017). Southern Ocean Phytoplankton in a Changing Climate. Front. Mar. Sci. 4:40. doi: 10.3389/fmars.2017.00040.

Dutkiewicz, S., Hickman, A. E., Jahn, O., Gregg, W. W., C. B. Mouw, C. B., and M. J. Follows (2015) Capturing optically important constituents and properties in a marine biogeochemical and ecosystem model Biogeosciences, 12, 4447–4481.

Hirata, T., Hardman-Mountford, N., Brewin, R., Aiken, J., Barlow, R., Suzuki, K., et al. (2011). Synoptic relationships between surface chlorophyll-a and diagnostic pigments specific to phytoplankton functional types. Biogeosciences 8, 311–327. doi: 10.5194/bg-8-311-2011.

Longhurst. A. (1998) Ecological Geography of the Sea, Academic press.

Losa, S. N., Soppa, M. A., Dinter, T., Wolanin A., Brewin R. J. W., Bricaud A., Oelker, J., Peeken I., Gentili B., Rozanov V. V., Bracher, A. (2017). Synergistic exploitation of hyper- and multispectral Sentinel measurements to determine Phytoplankton Functional Types (SynSenPFT), *Frontiers in Marine Science,* 4, 203. Doi: 10.3389/fmars.2017.00203.

Losa, S., Soppa, M. A., Dinter, T., Wolanin A., Brewin R. J. W., Bricaud A., Oelker, J., Peeken I., Gentili B., Rozanov V. V., Bracher, A. (2017): Global chlorophyll "a" surface concentrations for diatoms, coccolithophores and cyanobacteria as the synergistic SynSenPFT product combined PhytoDOAS and OC-PFT for the period of time August 2002 - April 2012, https://doi.org/10.1594/PANGAEA.875873.

Losa, S. N., Vezina, A., Wright, D., Lu, Y., Thompson, K. and Dowd, M. (2006) 3D ecosystem modelling in the North Atlantic: relative impacts of physical and biological parameterizations, Journal of marine systems, 61 (3), 230–245.

Menemenlis, D., Campin, J.-M., Heimbach, P., Hill, C., Lee, T., Nguyen, A., Schodlock, M., and H. Zhang (2008). High resolution global ocean and sea ice data synthesis (2008) Mercator Ocean Quartely Newsletter, 31, 13–21.

MITgcm Group (2012), MITgcm Manual, Online documentation, MIT/EAPS, Cambridge, MA 02139, USA.

Moisan, T. A. and Mitchell, B. G. (2018): Modeling Net Growth of Phaeocystis antarctica Based on Physiological and Optical Responses to Light and Temperature Co-limitation. Front. Mar. Sci. 4:437. doi: 10.3389/fmars.2017.00437.

Popova, E.E.; Pollard, R.T.; Lucas, M.I.; Venables, H.J.; Anderson, T.R. (2007): Real-time forecasting of ecosystem dynamics during the CROZEX experiment and the roles of light, iron, silicate, and circulation. Deep-Sea Research II, 54 (18-20), doi: 1966-1988.10.1016/j.dsr2.2007.06.018.

Quéguiner, B. (2013), Iron fertilization and the structure of planktonic communities in high nutrient regions of the Southern Ocean, Deep Sea Research Part II: Topical Studies in Oceanography, 90: 43–54, doi: 10.1016/j.dsr2.2012.07.024.

Sadeghi, A., Dinter, T., Vountas, M., Taylor, B. B., Altenburg-Soppa, M., Peeken, I., and A. Bracher (2012) Improvements to the PhytoDOAS method for identification of coccolithophores using hyperspectral satellite data. Ocean Sciences 8:1055-1070.

Signorini, S. R., V. M. T. Garcia, A. R. Piola, C. A. E. Garcia, M. M. Mata, *and* C. R. McClain *(*2006*)*, Seasonal and interannual variability of calcite in the vicinity of the Patagonian shelf break (38°S–52°S), Geophys. Res. Lett., 33, L16610, doi*:*10.1029/2006GL026592**.**

Smith et al. (2017) The influence of the environmental variability on the biogeography of coccolithophores and diatoms in the Great Calcite Belt, Biogeosciences, 14, 4905–4925 and diatoms in the Great Calcite Belt, Biogeosciences, 14, 4905–4925.

Soppa, M. A., Hirata, T., Silva, B., Dinter, T., Peeken, I., Wiegmann, S., Bracher, A. (2014) Global Retrieval of Diatom Abundance Based on Phytoplankton Pigments and Satellite Data. Remote Sensing, 6(10), 10089–10106.

Soppa, M. A., Peeken, I., and Bracher, A. (2017). Global chlorophyll “a” concentrations for diatoms, haptophytes and prokaryotes obtained with the Diagnostic Pigment Analysis of HPLC data compiled from several databases and individual cruises. doi:10.1594/PANGAEA.875879

Soppa, M., Völker, C. and Bracher, A. (2016): Diatom Phenology in the Southern Ocean: Mean Patterns, Trends and the Role of Climate Oscillations, Remote Sensing, 8 (420), pp. 1–17.
Taylor M. H., Losch M., Bracher, A. (2013) On the drivers of phytoplankton blooms in the Antarctic seasonal ice zone: a modelling approach. J. Geophys. Res. – Oceans 188: 63–75.
Tréguer, P., Bowler, C., Moriceau, B., Dutkiewicz, S., Gehlen, M., Aumont, O., Bittner, L., Dugdale, R., Finkel, Z., Iudicone, D., Jahn, O., Guidi, L., Lasbleiz, M., Leblanc, K., Levy, M., Pondaven, P. (2018) Influence of diatom diversity on the ocean biological carbon pump, Nature Geoscience, II (1): 27–37, doi: 10.1038/s41561-017-0028-x.

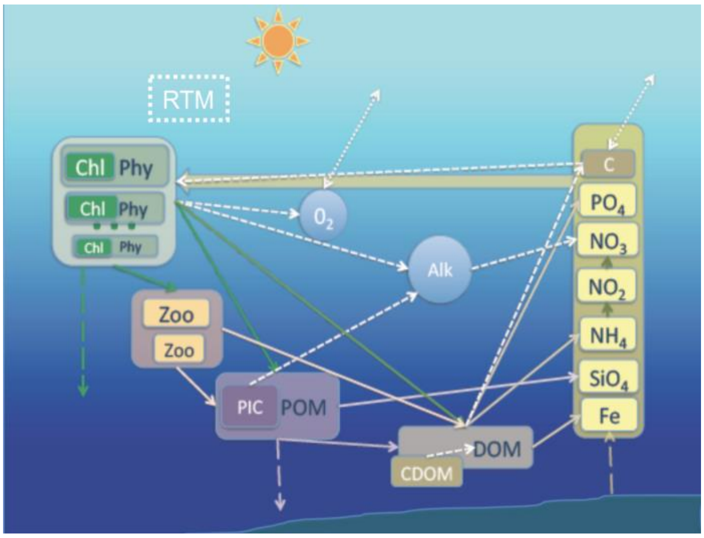

Figure1: The schematic diagram of the Darwin biogeochemical model (produced in accordance with the model description by Dutkiewicz et al., 2015).

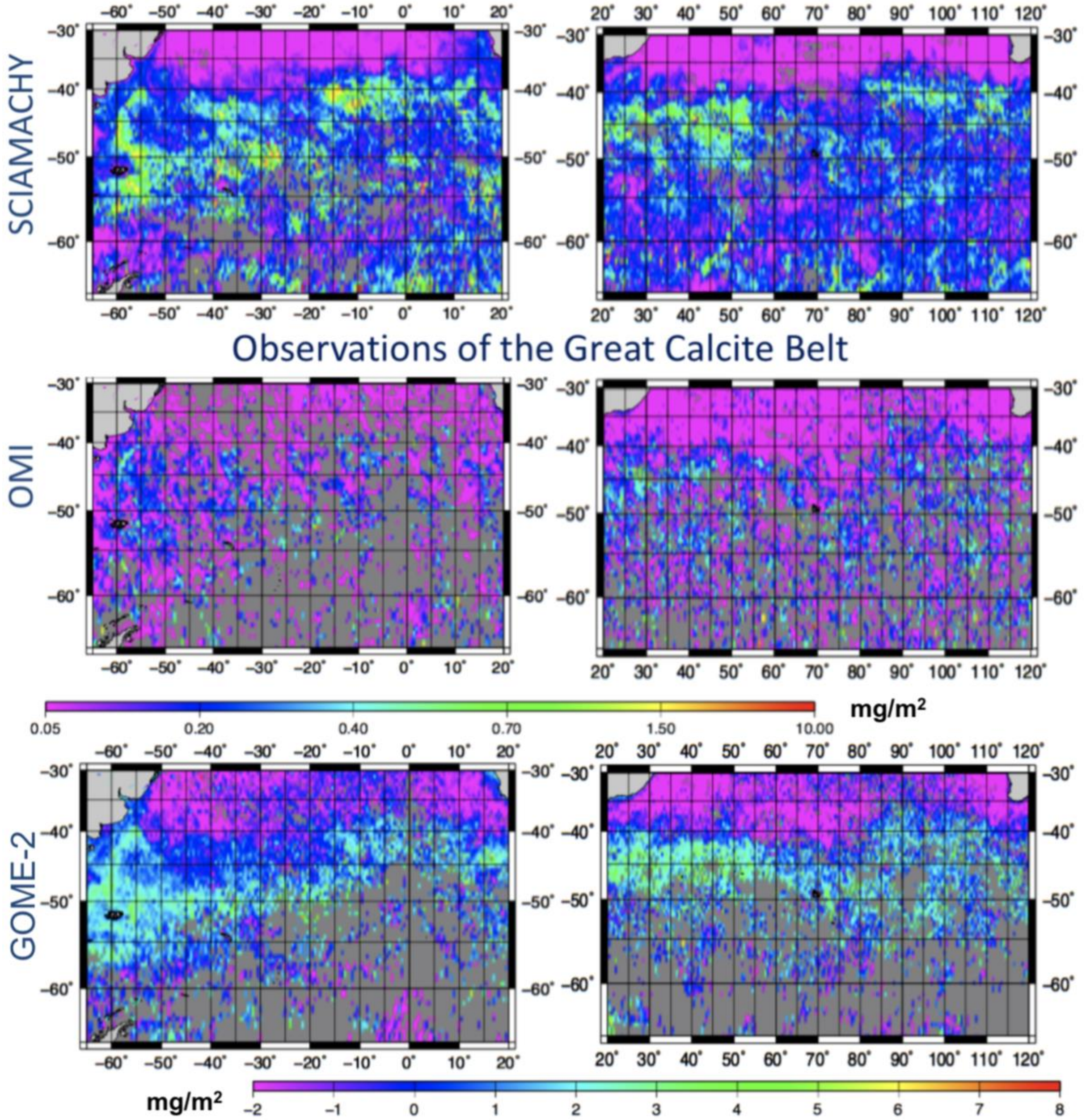

Figure 2: Comparison of coccolithophores fit factor retrieved for the Great Calcite Belt from SCIAMACHY, OMI and GOME-2 hyper-spectral information and averaged over the time period 17 January – 17 February 2011 (left panels) and 18 February – 20 March 2012 (right panels). The fit factor provides a measure of the respective PFT Chla within the observed light path. It varies from sensor to sensor depending on its respective solar zenith angle.

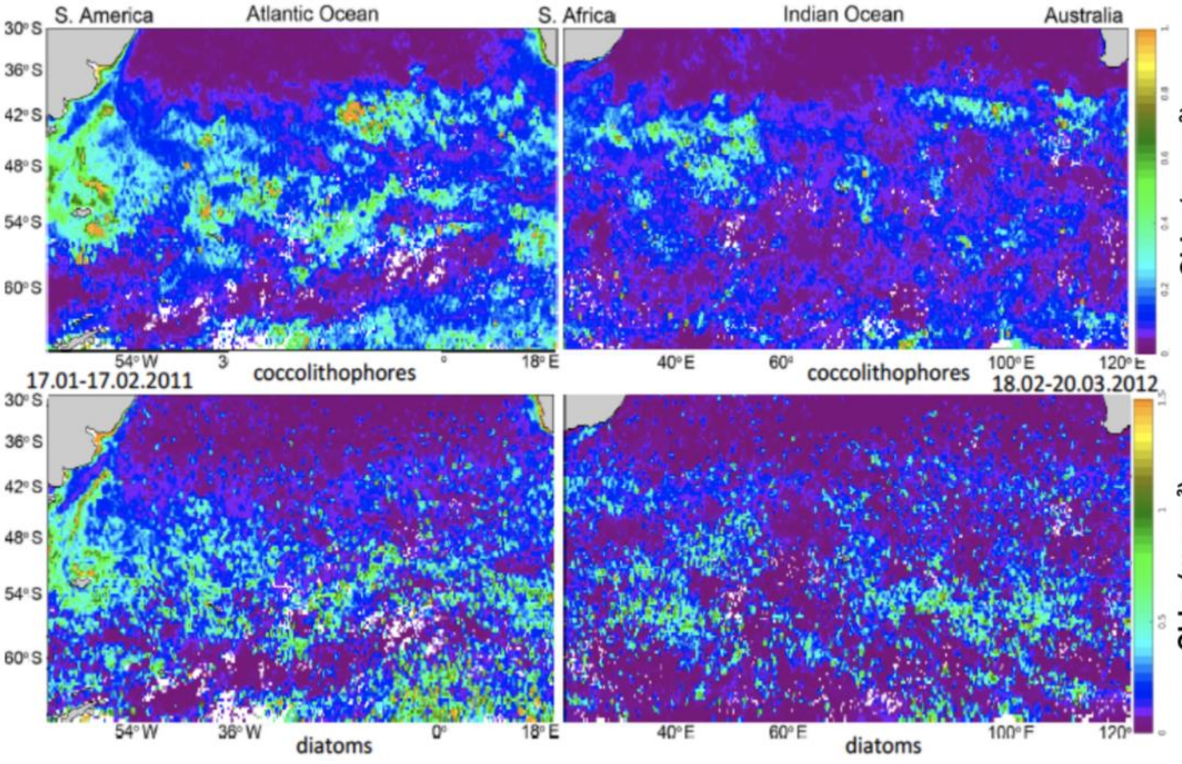

Figure 3: SynSenPFT Chlorophyll "a" concentration for coccolithophores (upper panels) and diatoms (bottom panels) in the Great Calcite Belt, averaged over the time period 17 January – 17 February 2011 (left panels) and 18 February – 20 March 2012 (right panels).

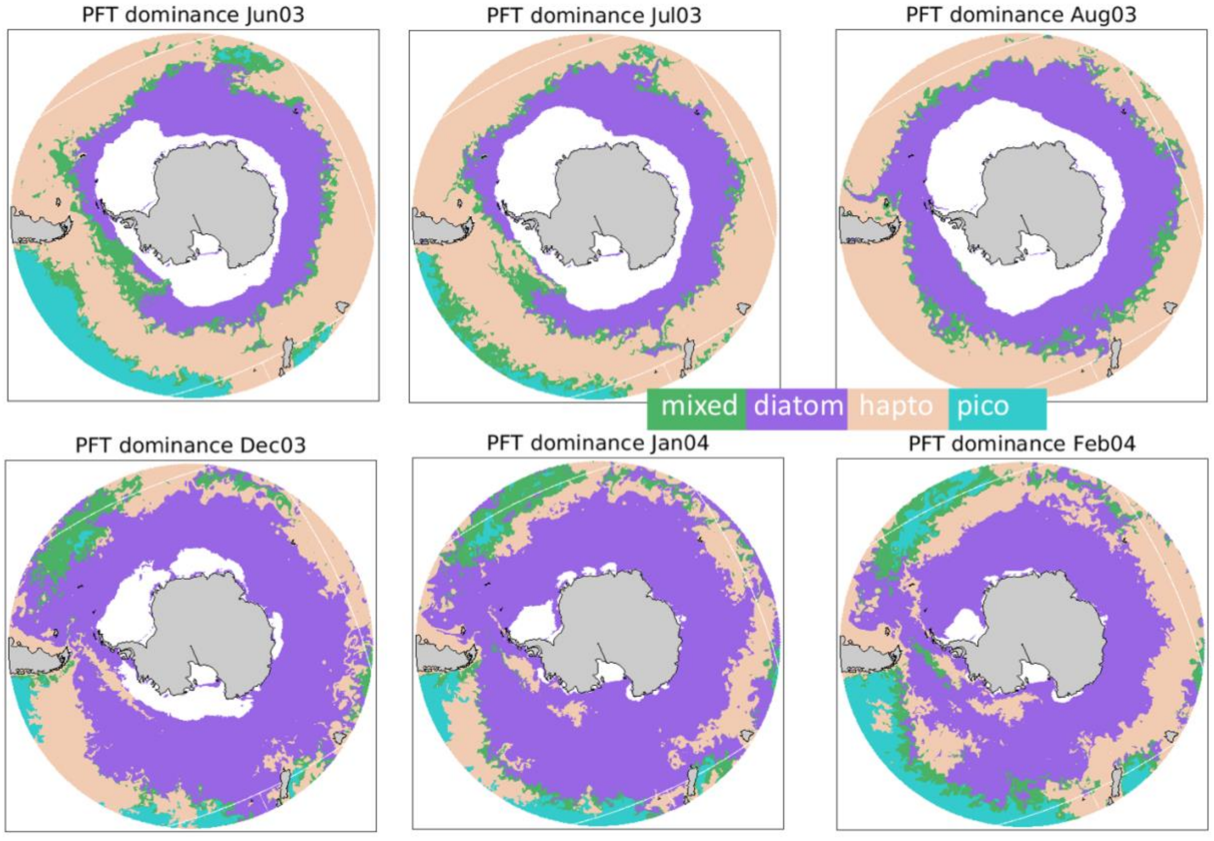

Figure 4: PFT dominance simulated with Darwin-MITgcm for 2003/2004, which is in a good agreement with the PFT dominance provided by PHYSAT satellite data product (http://log.cnrs.fr/Physat-2?lang=fr; Alvain et al. 2008). Pico – represents prochlorophytes.

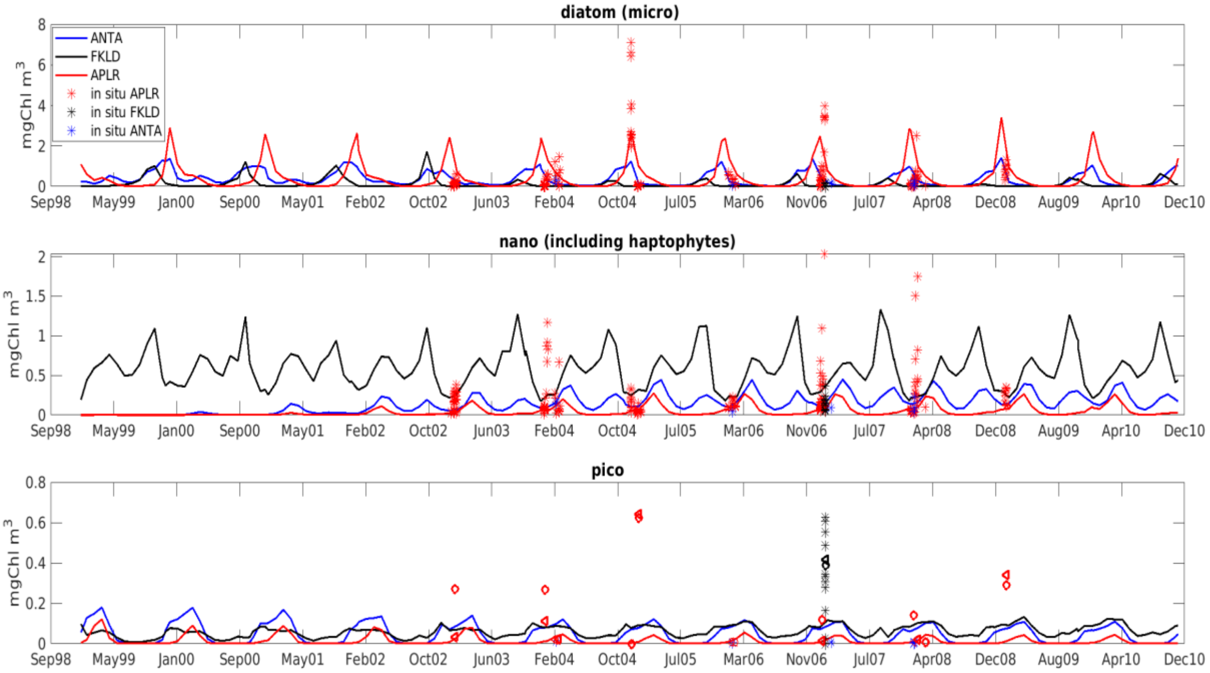

Figure 5: Model temporal evolution of PFTs chlorophyll *"a"* concentration for 3 biogeochemical provinces (Longhurst, 1998): Antarctic Province (ANTA), Austral Polar Province (APLR) and Southwest Atlantic Shelves Province (FKLD). Red circles represent mean, red triangles are median.

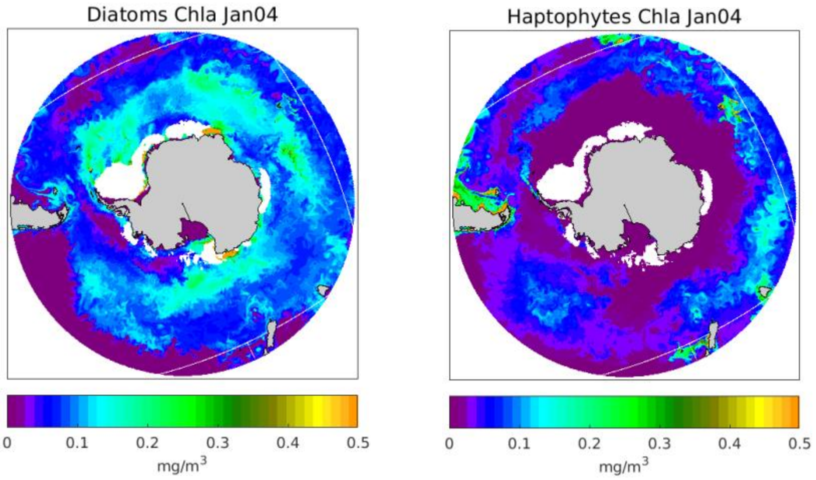

Figure 6: Spatial distribution of the diatoms and haptophytes chlorophyll *"a"* in the Southern Ocean (including the Great Calcite Belt) for January 2004.